DESY–08–089
ZEUS-pub-08-005
July 2008

arXiv:0807.0589v3 [hep-ex] 9 Jan 2009

Search for events with an isolated lepton and missing transverse momentum and a measurement of W production at HERA

ZEUS Collaboration

Abstract

A search for events with an isolated high-energy lepton and large missing transverse momentum has been performed with the ZEUS detector at HERA using a total integrated luminosity of $504\,\mathrm{pb}^{-1}$. The results agree well with Standard Model predictions. The cross section for production of single W bosons in electron-proton collisions with unpolarised electrons is measured to be $0.89^{+0.25}_{-0.22}\,(\mathrm{stat.})\,\pm 0.10\,(\mathrm{syst.})\,\mathrm{pb}$.

The ZEUS Collaboration

S. Chekanov, M. Derrick, S. Magill, B. Musgrave, D. Nicholass[1], J. Repond, R. Yoshida
Argonne National Laboratory, Argonne, Illinois 60439-4815, USA [n]

M.C.K. Mattingly
Andrews University, Berrien Springs, Michigan 49104-0380, USA

P. Antonioli, G. Bari, L. Bellagamba, D. Boscherini, A. Bruni, G. Bruni, F. Cindolo, M. Corradi, G. Iacobucci, A. Margotti, R. Nania, A. Polini
INFN Bologna, Bologna, Italy [e]

S. Antonelli, M. Basile, M. Bindi, L. Cifarelli, A. Contin, S. De Pasquale[2], G. Sartorelli, A. Zichichi
University and INFN Bologna, Bologna, Italy [e]

D. Bartsch, I. Brock, H. Hartmann, E. Hilger, H.-P. Jakob, M. Jüngst, A.E. Nuncio-Quiroz, E. Paul, U. Samson, V. Schönberg, R. Shehzadi, M. Wlasenko
Physikalisches Institut der Universität Bonn, Bonn, Germany [b]

N.H. Brook, G.P. Heath, J.D. Morris
H.H. Wills Physics Laboratory, University of Bristol, Bristol, United Kingdom [m]

M. Capua, S. Fazio, A. Mastroberardino, M. Schioppa, G. Susinno, E. Tassi
Calabria University, Physics Department and INFN, Cosenza, Italy [e]

J.Y. Kim
Chonnam National University, Kwangju, South Korea

Z.A. Ibrahim, B. Kamaluddin, W.A.T. Wan Abdullah
Jabatan Fizik, Universiti Malaya, 50603 Kuala Lumpur, Malaysia [r]

Y. Ning, Z. Ren, F. Sciulli
Nevis Laboratories, Columbia University, Irvington on Hudson, New York 10027 [o]

J. Chwastowski, A. Eskreys, J. Figiel, A. Galas, M. Gil, K. Olkiewicz, P. Stopa, L. Zawiejski
The Henryk Niewodniczanski Institute of Nuclear Physics, Polish Academy of Sciences, Cracow, Poland [i]

L. Adamczyk, T. Bołd, I. Grabowska-Bołd, D. Kisielewska, J. Łukasik, M. Przybycień, L. Suszycki
Faculty of Physics and Applied Computer Science, AGH-University of Science and Technology, Cracow, Poland [p]

A. Kotański[3], W. Słomiński[4]
Department of Physics, Jagellonian University, Cracow, Poland

U. Behrens, C. Blohm, A. Bonato, K. Borras, R. Ciesielski, N. Coppola, S. Fang, J. Fourletova[5], A. Geiser, P. Göttlicher[6], J. Grebenyuk, I. Gregor, T. Haas, W. Hain, A. Hüttmann, F. Januschek, B. Kahle, I.I. Katkov, U. Klein[7], U. Kötz, H. Kowalski, E. Lobodzinska, B. Löhr, R. Mankel, I.-A. Melzer-Pellmann, S. Miglioranzi, A. Montanari, T. Namsoo, D. Notz[8], A. Parenti, L. Rinaldi[9], P. Roloff, I. Rubinsky, R. Santamarta[10], U. Schneekloth, A. Spiridonov[11], D. Szuba[12], J. Szuba[13], T. Theedt, G. Wolf, K. Wrona, A.G. Yagües Molina, C. Youngman, W. Zeuner[8]
Deutsches Elektronen-Synchrotron DESY, Hamburg, Germany

V. Drugakov, W. Lohmann, S. Schlenstedt
Deutsches Elektronen-Synchrotron DESY, Zeuthen, Germany

G. Barbagli, E. Gallo
INFN Florence, Florence, Italy [e]

P. G. Pelfer
University and INFN Florence, Florence, Italy [e]

A. Bamberger, D. Dobur, F. Karstens, N.N. Vlasov[14]
Fakultät für Physik der Universität Freiburg i.Br., Freiburg i.Br., Germany [b]

P.J. Bussey[15], A.T. Doyle, W. Dunne, M. Forrest, M. Rosin, D.H. Saxon, I.O. Skillicorn
Department of Physics and Astronomy, University of Glasgow, Glasgow, United Kingdom [m]

I. Gialas[16], K. Papageorgiu
Department of Engineering in Management and Finance, Univ. of Aegean, Greece

U. Holm, R. Klanner, E. Lohrmann, P. Schleper, T. Schörner-Sadenius, J. Sztuk, H. Stadie, M. Turcato
Hamburg University, Institute of Exp. Physics, Hamburg, Germany [b]

C. Foudas, C. Fry, K.R. Long, A.D. Tapper
Imperial College London, High Energy Nuclear Physics Group, London, United Kingdom [m]

T. Matsumoto, K. Nagano, K. Tokushuku[17], S. Yamada, Y. Yamazaki[18]
Institute of Particle and Nuclear Studies, KEK, Tsukuba, Japan [f]

A.N. Barakbaev, E.G. Boos, N.S. Pokrovskiy, B.O. Zhautykov
Institute of Physics and Technology of Ministry of Education and Science of Kazakhstan, Almaty, Kazakhstan

V. Aushev[19], O. Bachynska, M. Borodin, I. Kadenko, A. Kozulia, V. Libov, M. Lisovyi, D. Lontkovskyi, I. Makarenko, Iu. Sorokin, A. Verbytskyi, O. Volynets
Institute for Nuclear Research, National Academy of Sciences, Kiev and Kiev National University, Kiev, Ukraine

D. Son
Kyungpook National University, Center for High Energy Physics, Daegu, South Korea [g]

J. de Favereau, K. Piotrzkowski
Institut de Physique Nucléaire, Université Catholique de Louvain, Louvain-la-Neuve, Belgium [q]

F. Barreiro, C. Glasman, M. Jimenez, L. Labarga, J. del Peso, E. Ron, M. Soares, J. Terrón, M. Zambrana
Departamento de Física Teórica, Universidad Autónoma de Madrid, Madrid, Spain [l]

F. Corriveau, C. Liu, J. Schwartz, R. Walsh, C. Zhou
Department of Physics, McGill University, Montréal, Québec, Canada H3A 2T8 [a]

T. Tsurugai
Meiji Gakuin University, Faculty of General Education, Yokohama, Japan [f]

A. Antonov, B.A. Dolgoshein, D. Gladkov, V. Sosnovtsev, A. Stifutkin, S. Suchkov
Moscow Engineering Physics Institute, Moscow, Russia [j]

R.K. Dementiev, P.F. Ermolov [†], L.K. Gladilin, Yu.A. Golubkov, L.A. Khein, I.A. Korzhavina, V.A. Kuzmin, B.B. Levchenko[20], O.Yu. Lukina, A.S. Proskuryakov, L.M. Shcheglova, D.S. Zotkin
Moscow State University, Institute of Nuclear Physics, Moscow, Russia [k]

I. Abt, A. Caldwell, D. Kollar, B. Reisert, W.B. Schmidke
Max-Planck-Institut für Physik, München, Germany

G. Grigorescu, A. Keramidas, E. Koffeman, P. Kooijman, A. Pellegrino, H. Tiecke, M. Vázquez[8], L. Wiggers
NIKHEF and University of Amsterdam, Amsterdam, Netherlands [h]

N. Brümmer, B. Bylsma, L.S. Durkin, A. Lee, T.Y. Ling
Physics Department, Ohio State University, Columbus, Ohio 43210 [n]

P.D. Allfrey, M.A. Bell, A.M. Cooper-Sarkar, R.C.E. Devenish, J. Ferrando, B. Foster, K. Korcsak-Gorzo, K. Oliver, A. Robertson, C. Uribe-Estrada, R. Walczak
Department of Physics, University of Oxford, Oxford United Kingdom [m]

A. Bertolin, F. Dal Corso, S. Dusini, A. Longhin, L. Stanco
INFN Padova, Padova, Italy [e]

P. Bellan, R. Brugnera, R. Carlin, A. Garfagnini, S. Limentani
Dipartimento di Fisica dell' Università and INFN, Padova, Italy [e]

B.Y. Oh, A. Raval, J. Ukleja[21], J.J. Whitmore[22]
Department of Physics, Pennsylvania State University, University Park, Pennsylvania 16802 [o]

Y. Iga
Polytechnic University, Sagamihara, Japan [f]

G. D'Agostini, G. Marini, A. Nigro
Dipartimento di Fisica, Università 'La Sapienza' and INFN, Rome, Italy [e]

J.E. Cole[23], J.C. Hart
Rutherford Appleton Laboratory, Chilton, Didcot, Oxon, United Kingdom [m]

H. Abramowicz[24], R. Ingbir, S. Kananov, A. Levy, A. Stern
Raymond and Beverly Sackler Faculty of Exact Sciences, School of Physics, Tel Aviv University, Tel Aviv, Israel [d]

M. Kuze, J. Maeda
Department of Physics, Tokyo Institute of Technology, Tokyo, Japan [f]

R. Hori, S. Kagawa[25], N. Okazaki, S. Shimizu, T. Tawara
Department of Physics, University of Tokyo, Tokyo, Japan [f]

R. Hamatsu, H. Kaji[26], S. Kitamura[27], O. Ota[28], Y.D. Ri
Tokyo Metropolitan University, Department of Physics, Tokyo, Japan [f]

M. Costa, M.I. Ferrero, V. Monaco, R. Sacchi, A. Solano
Università di Torino and INFN, Torino, Italy [e]

M. Arneodo, M. Ruspa
Università del Piemonte Orientale, Novara, and INFN, Torino, Italy [e]

S. Fourletov[5], J.F. Martin, T.P. Stewart
Department of Physics, University of Toronto, Toronto, Ontario, Canada M5S 1A7 [a]

S.K. Boutle[16], J.M. Butterworth, C. Gwenlan[29], T.W. Jones, J.H. Loizides, M. Wing[30]
Physics and Astronomy Department, University College London, London, United Kingdom [m]

B. Brzozowska, J. Ciborowski[31], G. Grzelak, P. Kulinski, P. Łużniak[32], J. Malka[32], R.J. Nowak, J.M. Pawlak, T. Tymieniecka, A. Ukleja, A.F. Żarnecki
Warsaw University, Institute of Experimental Physics, Warsaw, Poland

M. Adamus, P. Plucinski[33]
Institute for Nuclear Studies, Warsaw, Poland

Y. Eisenberg, D. Hochman, U. Karshon
Department of Particle Physics, Weizmann Institute, Rehovot, Israel [c]

E. Brownson, T. Danielson, A. Everett, D. Kçira, D.D. Reeder, P. Ryan, A.A. Savin, W.H. Smith, H. Wolfe
Department of Physics, University of Wisconsin, Madison, Wisconsin 53706, USA [n]

S. Bhadra, C.D. Catterall, Y. Cui, G. Hartner, S. Menary, U. Noor, J. Standage, J. Whyte
Department of Physics, York University, Ontario, Canada M3J 1P3 [a]

[1] also affiliated with University College London, United Kingdom
[2] now at University of Salerno, Italy
[3] supported by the research grant no. 1 P03B 04529 (2005-2008)
[4] This work was supported in part by the Marie Curie Actions Transfer of Knowledge project COCOS (contract MTKD-CT-2004-517186)
[5] now at University of Bonn, Germany
[6] now at DESY group FEB, Hamburg, Germany
[7] now at University of Liverpool, UK
[8] now at CERN, Geneva, Switzerland
[9] now at Bologna University, Bologna, Italy
[10] now at BayesForecast, Madrid, Spain
[11] also at Institut of Theoretical and Experimental Physics, Moscow, Russia
[12] also at INP, Cracow, Poland
[13] also at FPACS, AGH-UST, Cracow, Poland
[14] partly supported by Moscow State University, Russia
[15] Royal Society of Edinburgh, Scottish Executive Support Research Fellow
[16] also affiliated with DESY, Germany
[17] also at University of Tokyo, Japan
[18] now at Kobe University, Japan
[19] supported by DESY, Germany
[20] partly supported by Russian Foundation for Basic Research grant no. 05-02-39028-NSFC-a
[21] partially supported by Warsaw University, Poland
[22] This material was based on work supported by the National Science Foundation, while working at the Foundation.
[23] now at University of Kansas, Lawrence, USA
[24] also at Max Planck Institute, Munich, Germany, Alexander von Humboldt Research Award
[25] now at KEK, Tsukuba, Japan
[26] now at Nagoya University, Japan
[27] member of Department of Radiological Science, Tokyo Metropolitan University, Japan
[28] now at SunMelx Co. Ltd., Tokyo, Japan
[29] PPARC Advanced fellow
[30] also at Hamburg University, Inst. of Exp. Physics, Alexander von Humboldt Research Award and partially supported by DESY, Hamburg, Germany
[31] also at Łódź University, Poland
[32] member of Łódź University, Poland
[33] now at Lund Universtiy, Lund, Sweden
[†] deceased

[a] supported by the Natural Sciences and Engineering Research Council of Canada (NSERC)

[b] supported by the German Federal Ministry for Education and Research (BMBF), under contract numbers 05 HZ6PDA, 05 HZ6GUA, 05 HZ6VFA and 05 HZ4KHA

[c] supported in part by the MINERVA Gesellschaft für Forschung GmbH, the Israel Science Foundation (grant no. 293/02-11.2) and the U.S.-Israel Binational Science Foundation

[d] supported by the Israel Science Foundation

[e] supported by the Italian National Institute for Nuclear Physics (INFN)

[f] supported by the Japanese Ministry of Education, Culture, Sports, Science and Technology (MEXT) and its grants for Scientific Research

[g] supported by the Korean Ministry of Education and Korea Science and Engineering Foundation

[h] supported by the Netherlands Foundation for Research on Matter (FOM)

[i] supported by the Polish State Committee for Scientific Research, project no. DESY/256/2006 - 154/DES/2006/03

[j] partially supported by the German Federal Ministry for Education and Research (BMBF)

[k] supported by RF Presidential grant N 8122.2006.2 for the leading scientific schools and by the Russian Ministry of Education and Science through its grant for Scientific Research on High Energy Physics

[l] supported by the Spanish Ministry of Education and Science through funds provided by CICYT

[m] supported by the Science and Technology Facilities Council, UK

[n] supported by the US Department of Energy

[o] supported by the US National Science Foundation. Any opinion, findings and conclusions or recommendations expressed in this material are those of the authors and do not necessarily reflect the views of the National Science Foundation.

[p] supported by the Polish Ministry of Science and Higher Education as a scientific project (2006-2008)

[q] supported by FNRS and its associated funds (IISN and FRIA) and by an Inter-University Attraction Poles Programme subsidised by the Belgian Federal Science Policy Office

[r] supported by the Malaysian Ministry of Science, Technology and Innovation/Akademi Sains Malaysia grant SAGA 66-02-03-0048

1 Introduction

The production of W bosons in electron[1]-proton (ep) collisions is an interesting Standard Model (SM) process with a small cross section. This process, with subsequent leptonic decay of the W boson, also constitutes one of the most important SM backgrounds to many new physics searches [1, 2], for which high-energy leptons and large missing transverse momentum, $P_T^{\rm miss}$, are common signatures. Such searches have been performed previously by both the H1 [2–4] and ZEUS [1,5,6] collaborations. The H1 collaboration observed an excess of electron or muon events with large hadronic transverse momentum, P_T^X, over the SM predictions. Previous ZEUS results have not confirmed this excess.

This paper presents a new search and a measurement of the cross section for W production at HERA. The study was performed by selecting events containing isolated electrons or muons with high transverse momentum, P_T^l, in events with large $P_T^{\rm miss}$. The data used were taken from 1994 to 2007. The total integrated luminosity analysed was $504\,{\rm pb}^{-1}$, a four-fold increase compared to previous ZEUS searches [1,6].

2 Standard Model expectations

The SM predicts the production of single W and Z bosons in ep collisions at HERA. The event topology studied here is large $P_T^{\rm miss}$ and an isolated lepton with large P_T^l.

W production: $ep \to eWX$ or $ep \to \nu WX$
Neutral current W production, $ep \to eWX$, with subsequent leptonic decay, $W \to l\nu$, is the dominant SM process that produces events matching the desired topology. Charged current W production, $ep \to \nu WX$, with subsequent leptonic decay also produces such events.

The SM production cross section, obtained from a calculation including Quantum Chromodynamics (QCD) corrections at next-to-leading-order (NLO) [7, 8], is 1.1 pb and 1.3 pb for the relevant centre-of-mass energies, $\sqrt{s}$, of 300 GeV and 318 GeV respectively. The estimated uncertainty on this calculation is 15%. Monte Carlo (MC) events have been generated with the leading-order EPVEC generator [9] and weighted by a factor dependent on the transverse momentum and rapidity of the W, such that the resulting cross sections correspond to the NLO calculation [10]. The EPVEC MC is also used to generate $ep \to \nu_e WX$ events. The contribution of $ep \to \nu_e WX$ to the total W production cross section is approximately 7%.

[1] In this paper "electron" refers both to electrons and positrons unless stated otherwise.

Z production: $ep \to eZ(\to \nu\bar{\nu})X$
The process $ep \to eZ(\to \nu\bar{\nu})X$ can produce high-energy scattered electrons and large $P_T^{\rm miss}$. The visible cross section for this process as calculated by EPVEC is less than 3% of the predicted W production cross section. It was neglected in this analysis.

Several SM processes can produce events with large $P_T^{\rm miss}$ and high-energy leptons as a result of mismeasurements.

Neutral current deep inelastic scattering (NC DIS): $ep \to eX$
Genuine isolated high-energy electrons are produced in NC DIS. Together with a fake $P_T^{\rm miss}$ signal from mismeasurement, they form the dominant fake signal in searches for isolated electrons at high P_T^X. Neutral current DIS events were simulated using the generator DJANGO6 [11], an interface to the MC programs HERACLES 4.5 [12] and LEPTO 6.5 [13]. Leading-order electroweak radiative corrections were included and higher-order QCD effects were simulated using the colour-dipole model of ARIADNE 4.08 [14]. Hadronisation of the partonic final state was performed by JETSET [15].

Charged current deep inelastic scattering (CC DIS): $ep \to \nu X$
A CC DIS event can mimic the selected topology if it contains a fake electron as there is real $P_T^{\rm miss}$ due to the escaping neutrino. Charged current DIS events were simulated using the generator DJANGO6 as described for the NC DIS events.

Lepton pair production: $ep \to el^+l^-X$
Lepton pair production can mimic the selected topology if one lepton escapes detection or measurement errors cause apparent missing momentum. Lepton pair production is the dominant fake signal in searches for isolated high-P_T muons. This process was simulated using the GRAPE [16] dilepton generator.

Photoproduction of jets: $\gamma p \to X$
Hard photoproduction processes can also contribute to the fake signal rate. This may occur when a particle from the hadronic final state is interpreted as an isolated lepton together with a fake $P_T^{\rm miss}$ signal arising from mismeasurement. Photoproduction processes as simulated with HERWIG 6.1 [17] make a negligible contribution to the SM expectation.

3 The ZEUS detector

A detailed description of the ZEUS detector can be found elsewhere [18]. Charged particles were tracked in the central tracking detector (CTD) [19] which operated in a magnetic field of 1.43 T provided by a thin superconducting solenoid. Before the 2003–2007 running

period, the ZEUS tracking system was upgraded with a silicon micro vertex detector (MVD) [20]. The high-resolution uranium–scintillator calorimeter (CAL) [21] consisted of three parts: the forward, the barrel and the rear calorimeters. The smallest subdivision of the CAL was called a cell. A three-level trigger was used to select events online [22] requiring large $P_T^{\rm miss}$ or well isolated electromagnetic deposits in the CAL.

4 Event reconstruction

Electrons were identified by an algorithm that selects candidate electromagnetic clusters in the CAL and combines them with tracking information. The algorithm was optimised for maximum electron-finding efficiency and electron-hadron separation for NC DIS events [23]. Electromagnetic clusters were classified as isolated electron candidates when the energy not associated with the cluster in an $\{\eta, \phi\}$ cone of radius 0.8 around the electron direction was less than 5 GeV and less than 5% of the electromagnetic cluster energy measured with the calorimeter, where $\eta = -\log(\tan(\theta/2))$.

Muons were identified through their signature as minimum ionising particles (MIPs). Their energy depositions can be spread over several calorimeter clusters. Therefore, neighbouring clusters were grouped together into larger-scale objects which, provided they passed topological and energy cuts, were classified as CAL MIPs. In this analysis a muon candidate was selected if a CAL MIP matched an extrapolated CTD track from the primary vertex to within 20 cm.

The missing transverse momentum was determined from calorimetric and tracking information. The magnitude of the missing transverse momentum measured with the CAL was defined as

$$P_T^{\rm CAL} = \sqrt{\left(\sum_i p_{X,i}^{\rm CAL}\right)^2 + \left(\sum_i p_{Y,i}^{\rm CAL}\right)^2},$$

where $p_{X,i}^{\rm CAL} = E_i \sin\theta_i \cos\phi_i$ and $p_{Y,i}^{\rm CAL} = E_i \sin\theta_i \sin\phi_i$ were calculated from individual energy deposits, E_i, in clusters of CAL cells corrected [24] for energy loss in inactive material. In $W \to e\nu$ events, $P_T^{\rm CAL}$ as defined above is an estimate of the missing transverse momentum carried by the neutrino, P_T^{ν}. In $W \to \mu\nu$ events, the muon deposits very little energy in the calorimeter and therefore a better estimate of P_T^{ν} can be obtained if the momentum of the muon is calculated from its track measured in the CTD ($p^{\mu,{\rm track}}$). Combination with the above estimate of the total transverse momentum from the calorimeter

leads to

$$P_T^{\rm miss} = \sqrt{\left(\sum_i p_{X,i}^{\rm CAL} + p_X^{\mu,{\rm track}}\right)^2 + \left(\sum_i p_{Y,i}^{\rm CAL} + p_Y^{\mu,{\rm track}}\right)^2}.$$

The hadronic transverse momentum, P_T^X, was defined as the sum over those calorimeter cells that are not assigned to lepton-candidate clusters.

The charged-lepton transverse momentum, P_T^l, was calculated from the calorimeter cluster for $l = e$ and from the track momentum for $l = \mu$. The transverse mass for W bosons decaying via $W \to l\nu$ is defined as:

$$M_T = \sqrt{2P_T^l P_T^\nu (1 - \cos\phi^{l\nu})},$$

where $\phi^{l\nu}$ is the azimuthal separation of the lepton and P_T^ν vectors.

The following event properties were used to suppress backgrounds from mismeasured large $P_T^{\rm miss}$ and fake high-energy leptons. Selection cuts on these event properties will be briefly described in Section 5.

The quantity ξ_e^2 was defined as

$$\xi_e^2 = 2E_e' E_e (1 + \cos\theta_e),$$

where E_e' is the energy of the final-state electron, $E_e = 27.5\,{\rm GeV}$ is the electron beam energy and θ_e is the polar angle of the electron measured in the calorimeter. For NC DIS events, where the scattered electron is identified as the isolated lepton, ξ_e^2 corresponds to the virtuality of the exchanged boson, Q^2. Neutral current DIS events generally have low values of ξ_e^2 whilst electrons from W decay will generally have high values of ξ_e^2.

The acoplanarity angle, $\phi_{\rm acop}$, is the azimuthal separation in the $\{X, Y\}$ plane of the outgoing lepton and the vector that balances the hadronic transverse momentum vector. For well measured NC DIS events, $\phi_{\rm acop}$ is close to zero.

The quantity $\frac{V_{\rm ap}}{V_{\rm p}}$ is defined as the ratio of anti-parallel to parallel components of the measured calorimeter transverse momentum with respect to its direction. It is a measure of the azimuthal balance of the event: events with one or more high-P_T particles that do not deposit energy in the calorimeter normally have low values of $\frac{V_{\rm ap}}{V_{\rm p}}$.

The quantity δ was defined as:

$$\delta = \sum_i E_i (1 - \cos\theta_i),$$

where the sum runs over energy deposits as with $P_T^{\rm CAL}$. Due to longitudinal momentum conservation, δ peaks at twice the electron beam energy for fully contained events. Values of δ much larger than $2E_e = 55$ GeV are usually caused by the superposition of a NC DIS event with additional energy deposits in the rear calorimeter not related to ep collisions.

5 Event selection

The data samples used in this analysis, the beam configurations and integrated luminosities, $\mathcal{L}$, are given in Table 1. From 2003 onwards, the electron beam was longitudinally polarised with average polarisation of approximately $\pm 30\%$. The amount of data with left- and right-handed electrons was approximately equal.

Offline, $P_T^{\rm CAL}$ and $P_T^{\rm miss}$ were required to be greater than 12 GeV. The value of $P_T^{\rm CAL}$ calculated excluding the inner ring of calorimeter cells around the forward beam-pipe hole also had to be greater than 9 GeV. These cuts were more stringent than the corresponding online trigger thresholds. Other preselection cuts were the requirement that the Z-coordinate of the tracking vertex be reconstructed within 50 cm (30 cm) of the nominal interaction point for 1994–2000 (2003–2007) data and that there was a track from this vertex associated with the lepton. Cuts on the calorimeter timing and algorithms based on the pattern of tracks were used to reject beam-gas, cosmic-ray and halo-muon events. After these preselection criteria were applied, events with isolated electrons and muons were selected separately using the criteria listed in Table 2. These criteria are described below.

In the search for isolated high-energy electrons, electromagnetic clusters were selected as described in Section 4. The distance of closest approach of the track associated with the electromagnetic cluster was required to be less than 10 cm. Since most fake electrons are misidentified hadrons close to jets, the fake signal was further reduced by requiring that the electron track be separated by a distance, $D_{\rm track}$, of at least 0.5 units in $\{\eta, \phi\}$ space from other "good" tracks in the event. A track was labelled good if it had momentum larger than 0.2 GeV, was associated with the event vertex and lay within $15^\circ < \theta < 164^\circ$. To maintain efficiency in the forward region, this track isolation cut was not used for $\theta_e < 45^\circ$. Requiring that the matching electron track have transverse momentum greater than 5 GeV also removed fake electrons. The isolated electrons were required to have $P_T^e > 10$ GeV and lie within the region $15^\circ < \theta_e < 120^\circ$. The fake signal rate from NC DIS was strongly suppressed by requiring $5 < \delta < 50$ GeV and further suppressed by requiring that $\phi_{\rm acop} > 20^\circ$ for events that have a well defined P_T^X, i.e. larger than 1 GeV (otherwise no acoplanarity angle cut was applied). In addition, for low values of $P_T^{\rm CAL}$ (< 25 GeV), where NC DIS events dominate, ξ_e^2 was required to be greater than 5000 GeV^2. A P_T^e-dependent cut on $\frac{V_{\rm ap}}{V_{\rm p}}$ was applied.

In the search for isolated muons, the muon candidate was required to be isolated by a distance, $D_{\rm jet}$, of at least one unit in $\{\eta, \phi\}$ space from any jet with $E_T^{\rm jet} > 5$ GeV and $-3 < \eta^{\rm jet} < 3$. The fake signal rate was reduced by requiring that $D_{\rm track}$ be at least 0.5. Events containing such isolated muon candidates with $P_T^\mu > 1$ GeV were excluded from the isolated-electron search. Events in which more than one isolated muon with

$P_T^\mu > 1\,\text{GeV}$ were found were rejected. The cut $\delta < 70\,\text{GeV}$ removed superpositions of NC DIS events with non-ep energy deposits in the RCAL . The muon was required to lie in the phase space $P_T^\mu > 10\,\text{GeV}$ and $15^\circ < \theta_\mu < 120^\circ$. Cuts on ϕ_{acop} and $\frac{V_{\text{ap}}}{V_{\text{p}}}$ were applied to reduce the fake signal rate from dilepton production. The quantity P_T^X was required to be greater than 12 GeV.

6 Systematic uncertainties

The major experimental sources of systematic uncertainty on the number of events expected from SM processes originated from the luminosity measurement, the calorimeter energy scale and the simulation of processes in the extremities of phase space. Uncertainties on the expectation for the observed rate of W production arising from lepton identification were negligible for the electron search and $\pm 5\%$ for the muon search.

The uncertainties on the luminosity measurements gave an overall uncertainty of approximately $\pm 2.9\%$ ($\pm 3.4\%$) on the expected SM event rate for e^+p (e^-p) data.

The uncertainty on the CAL energy scale was investigated by globally scaling energy as measured in the electromagnetic section of the calorimeter (EMC) by $\pm 2\%$. The shifts in the expectations in the different P_T^X bins were $\pm(0.5\text{–}3.5)\%$ in the electron search while they were negligible for the muon search. The hadronic energy-scale uncertainty was varied by globally scaling energy as measured in the hadronic section of the calorimeter by $\pm 3\%$. The effect on the SM prediction was $\pm(2\text{–}5)\%$ in both the electron and muon searches.

Alternative event samples were used to verify that the fake signal rates were well simulated by the MC. The contribution of NC DIS to the electron search was studied by selecting a sample of isolated electrons in the phase space $\theta_e < 120^\circ$, $P_T^e > 10$ GeV and $P_T^{\text{CAL}} > 12$ GeV. The fraction of the sample arising from NC DIS was enhanced by applying in addition the requirement that $\delta > 30$ GeV and that $\phi_{\text{acop}} < 17^\circ$. A systematic uncertainty of $\pm 15\%$ on the fake signal rate from NC was determined from the level of agreement between data and MC for this selection. The effect of this uncertainty on the SM prediction was $\pm(1\text{–}4)\%$ for the electron search and was negligible in the muon search.

The contribution from CC DIS to the electron search arises mainly from fake isolated electron candidates originating from the hadronic system. To assess the ability of the MC to reproduce these events, a sample of NC DIS candidates with additional electron candidates other than the scattered DIS electron was selected. The additional electrons were required to be isolated according to the same isolation criteria as used in the isolated-lepton search. The phase space of the additional electron was $\theta_e < 120^\circ$ and $P_T^e > 10$ GeV. From the agreement between data and MC, a systematic uncertainty of $\pm 25\%$

was determined for the fake signal rate from CC. The effect of this uncertainty on the SM prediction was ±(2–8)% for the electron search and was negligible in the muon search.

Dilepton events produce a significant fake signal rate in the isolated muon search. A dimuon enriched sample was selected in the phase space $P_T^{\rm CAL} > 12$ GeV, $P_T^{\mu} > 10$ GeV and $5^\circ < \theta_\mu < 120^\circ$. The dimuon component was enhanced by requiring that $\phi_{\rm acop} < 20^\circ$ and $\frac{V_{\rm ap}}{V_{\rm p}} < 0.2$. An uncertainty of ±25% on the dilepton fake signal rate was determined from the level of agreement between data and MC. The effect of this uncertainty on the SM prediction was ±(4–6)% for the muon search and was negligible in the electron search.

The theoretical uncertainty of ±15% on the W production cross section gave the largest uncertainty on the total SM prediction in both searches, being approximately ±12% in the muon search and ±(8–12)% for the electron search.

The total systematic uncertainty on the SM prediction was obtained by summing all of the individual effects in quadrature. It was ±(11–13)% for the various P_T^X bins in the electron search and was ±(14–15%) in the muon search.

7 Isolated-lepton search results

Distributions of θ_e, P_T^e, M_T, $\phi_{\rm acop}$, P_T^X and $P_T^{\rm CAL}$ for the isolated electron sample are compared to the expectation from the MC simulation normalised to the luminosity in Fig. 1. The data are well described by the SM Monte Carlo predictions. This is also the case when the data are separated into e^+p collision and e^-p collision samples. The expectation from the SM and the fraction arising from W production, in bins of P_T^X for the electron search are given in Table 3. No significant excess over the SM predictions is observed.

Distributions of θ_μ, P_T^μ, $\phi_{\rm acop}$ and P_T^X for the isolated muon sample are compared to the expectation from the MC simulation normalised to the luminosity in Fig. 2. The data are well described by the SM Monte Carlo predictions. This is also the case when the data are separated into e^+p collision and e^-p collision samples. The expectation from the SM and the fraction arising from W production, in bins of P_T^X, are given in Table 4.

The muon and electron search results are combined in Table 5. No excess over the SM predictions is observed. The good agreement between the SM predictions and observed data makes it possible to extract the W production cross section.

8 Extraction of W production cross section

In order to enhance the fraction of events from W production in the electron search, an additional requirement of $\theta_e < 90^\circ$ was applied to the sample of Section 5. For $e^- p$ ($e^+ p$) collisions, this cut removed 3 (3) events from data compared to an SM expectation of 2.6 (2.5). This final sample and the μ sample from Section 5 were used to measure the cross section for the process $ep \to lWX$ assuming a branching fraction, $\mathcal{BR}$ ($W \to l\nu_l$), of 10.8 % [25] per lepton. The EPVEC MC reweighted as described in Section 2 was used in the unfolding process to calculate acceptances.

In the $W \to e\nu_e$ channel, the measured phase space is $15^\circ < \theta_e < 90^\circ$, $P_T^e > 10$ GeV and $P_T^{\rm miss} > 12$ GeV. In the $W \to \mu\nu_\mu$ channel, the measured phase space is $15^\circ < \theta_\mu < 120^\circ$, $P_T^\mu > 10$ GeV, $P_T^{\rm miss} > 12$ GeV and $P_T^X > 12$ GeV. The efficiency in the measured phase space in the $W \to e\nu_e$ ($W \to \mu\nu_\mu$) channel is 55% (40%). The total acceptance, A_i, for each channel is given by an extrapolation factor from the measured phase space to the full $ep \to lWX$ phase space multiplied by the efficiency for reconstructing an event within the measured phase space. The acceptance for the $W \to e\nu_e$ ($W \to \mu\nu_\mu$) channel was 33% (11%). The small contribution from $W \to \tau\nu_\tau$ decays was taken into account.

The cross section was determined from the likelihood for observing n_i events in each search channel, defined by:

$$L(\sigma) = \prod_i \left(\alpha_i \int_0^\infty dx G_i(x) \frac{e^{(-x)} x^{n_i}}{(n_i!)} \right),$$

where the product runs over all samples being combined and $G_i(x)$ is a Gaussian function centred on m_i with width δ_i; $m_i = b_i(x) + A_i \mathcal{BR}_i \mathcal{L} \sigma$, where b_i is the number of events expected from the background and $\mathcal{BR}_i$ is the branching ratio for the channel. The quantity δ_i is the statistical uncertainty on the background prediction and $\alpha_i = (\int_0^\infty dx G_i(x))^{-1}$. The measured value of the cross-section, $\sigma_{\rm meas}$, is that which minimises $-\ln L(\sigma)$. The upper and lower bounds on $\sigma_{\rm meas}$ are the values at which $-\ln L(\sigma) = -\ln L(\sigma_{\rm meas}) + 0.5$. Cross sections for the exclusive $W \to e\nu_e$ and $W \to \mu\nu_\mu$ decay channels were evaluated by combining $e^+ p$ and $e^- p$ samples in the same manner.

Systematic uncertainties on the extracted cross section were evaluated by considering the effects discussed in Section 6. In addition, the extrapolation factor for the muon channel is sensitive to the P_T^X distribution. In order to take this into account, the cross section in the $P_T^X < 12$ GeV region was varied by the theoretical uncertainty on the total cross section, $\pm 15\%$, leading to variations in the extrapolation factor of $\pm 9\%$. The variation observed on the combined cross section from this change was $\pm 3\%$. The systematic uncertainties from individual effects were added in quadrature. The dominant contribution to the total

systematic uncertainty came from the uncertainty on the fake signal rate from CC DIS; this contributed uncertainties of about $\pm 11\%$ ($\pm 5\%$) to the cross section for $e^- p$ ($e^+ p$) collisions.

The cross sections are given in Table 6. The cross section is given at the luminosity-weighted mean of $\sqrt{s}$ for the data samples used. The mean polarisation of the electron beam in the $e^- p$ and $e^+ p$ data sets is less than 3%. The effect of such levels of polarisation on the inclusive cross section, $\sigma_{ep \to lWX}$, is predicted by EPVEC to be less than 1% and was neglected. The cross section is therefore quoted for a mean polarisation of 0. When $e^+ p$ and $e^- p$ data are combined the cross section is quoted for the luminosity-weighted mean of the $e^+ p$ and $e^- p$ cross sections. The measured cross sections are consistent with the SM predictions. The statistical significance of the $\sigma_{ep \to lWX}$ measurement was evaluated by considering the probability of measuring an equal or larger cross section in data for a prediction containing no W production. When the sytematic uncertainties were (were not) taken into account this probability was 1.1×10^{-6} (1.1×10^{-7}), corresponding to a significance of 4.7σ (5.2σ). The full likelihood curve including both systematic and statistical uncertainties is available in Appendix A and from the ZEUS web page [26].

9 Summary

A search was made for isolated high-energy electrons and muons in events with large $P_T^{\rm miss}$, compatible with single W production with subsequent decay $W \to e\nu_e$ or $W \to \mu\nu_\mu$ in ep collisions at a centre-of-mass energy of about 320 GeV. A data sample with a total integrated luminosity of 504 pb^{-1} was used. The rate of production of such events at high hadronic transverse momentum was found to be consistent with the SM predictions. The excess in these types of events observed by the H1 collaboration is not confirmed. The total cross section for single W production was measured to be

$$\sigma_{ep \to lWX} = 0.89^{+0.25}_{-0.22}\,(\text{stat.}) \pm 0.10(\text{syst.})\,\text{pb},$$

consistent with SM predictions. The measurement represents a four-fold improvement in precision relative to the previously published ZEUS value. This measurement constitutes strong evidence for W production in ep collisions at HERA with a significance of 4.7σ.

Acknowledgements

We are grateful to the DESY directorate for their strong support and encouragement. We thank the HERA machine group whose outstanding efforts were essential for the successful

completion of this work. The design, construction and installation of the ZEUS detector were made possible by the efforts of many people not listed as authors.

References

[1] ZEUS Coll., S. Chekanov et al., Phys. Lett. **B 559**, 153 (2003).

[2] H1 Coll., V. Andreev et al., Phys. Lett. **B 561**, 241 (2003).

[3] H1 Coll., C. Adloff et al., Eur. Phys. J. **C 5**, 575 (1998).

[4] H1 Coll., A. Aktas et al., Eur. Phys. J. **C 48**, 699 (2006).

[5] ZEUS Coll., J. Breitweg et al., Phys. Lett. **B 471**, 411 (2000).

[6] ZEUS Coll., S. Chekanov et al., Phys. Lett. **B 583**, 41 (2003).

[7] K-P.O. Diener, C. Schwanenberger and M. Spira, Eur. Phys. J. **C 25**, 405 (2002).

[8] P. Nason, R. Rückl and M. Spira, J. Phys. **G 17**, 1443 (1999).

[9] U. Baur, J.A.M. Vermaseren and D. Zeppenfeld, Nucl. Phys. **B 375**, 3 (1992).

[10] K.-P.O. Diener, C. Schwanenberger and M. Spira, Preprint hep-ex/0302040, 2003.

[11] K. Charchula, G.A. Schuler and H. Spiesberger, Comp. Phys. Comm. **81**, 381 (1994).

[12] A. Kwiatkowski, H. Spiesberger and H.-J. Möhring, Comp. Phys. Comm. **69**, 155 (1992). Also in *Proc. Workshop Physics at HERA*, eds. W. Buchmüller and G.Ingelman, (DESY, Hamburg, 1991).

[13] G. Ingelman, A. Edin and J. Rathsman, Comp. Phys. Comm. **101**, 108 (1997).

[14] L. Lönnblad, Comp. Phys. Comm. **71**, 15 (1992).

[15] T. Sjöstrand, Comp. Phys. Comm. **39**, 347 (1986).

[16] T. Abe, Comp. Phys. Comm. **136**, 126 (2001).

[17] G. Marchesini et al., Comp. Phys. Comm. **67**, 465 (1992).

[18] ZEUS Coll., U. Holm (ed.), *The ZEUS Detector*. Status Report (unpublished), DESY (1993), available on `http://www-zeus.desy.de/bluebook/bluebook.html`.

[19] N. Harnew et al., Nucl. Inst. Meth. **A 279**, 290 (1989);
B. Foster et al., Nucl. Phys. Proc. Suppl. **B 32**, 181 (1993);
B. Foster et al., Nucl. Inst. Meth. **A 338**, 254 (1994).

[20] A. Polini et al., Nucl. Inst. Meth. **A 581**, 656 (2007).

[21] M. Derrick et al., Nucl. Inst. Meth. **A 309**, 77 (1991);
A. Andresen et al., Nucl. Inst. Meth. **A 309**, 101 (1991);
A. Caldwell et al., Nucl. Inst. Meth. **A 321**, 356 (1992);
A. Bernstein et al., Nucl. Inst. Meth. **A 336**, 23 (1993).

[22] W. H. Smith, K. Tokushuku and L. W. Wiggers, *Proc. Computing in High-Energy Physics (CHEP), Annecy, France, Sept. 1992*, C. Verkerk and W. Wojcik (eds.), p. 222. CERN, Geneva, Switzerland (1992). Also in preprint DESY 92-150B;
P. Allfrey, Nucl. Inst. Meth. **A 580**, 1257 (2007).

[23] ZEUS Coll., J. Breitweg et al., Z. Phys. **C 74**, 207 (1997).

[24] ZEUS Coll., J. Breitweg et al., Eur. Phys. J. **C 11**, 427 (1999).

[25] Particle Data Group, W.-M. Yao et al., J. Phys. **G 33**, 1 (2006).

[26] Available on `http://www-zeus.desy.de/physics/exo/ZEUS_PUBLIC/zeus-pub-08-005`.

Period	Beams	Electron energy (GeV)	Proton energy (GeV)	$\sqrt{s}$ (GeV)	$\mathcal{L}$ (pb^{-1})
1994–1997	e^+p	27.5	820	300	48.2
1998–1999	e^-p	27.5	920	318	16.7
1999–2000	e^+p	27.5	920	318	65.1
2003–2004	e^+p	27.5	920	318	40.8
2004–2006	e^-p	27.5	920	318	190.9
2006–2007	e^+p	27.5	920	318	142.4

Table 1: *Details of the different data subsamples over the 1994–2007 running period. From 2003 onwards the electron beam was longitudinally polarised.*

Variable	Electron	Muon
P_T^{CAL}	$> 12\,\mathrm{GeV}$	$> 12\,\mathrm{GeV}$
P_T^{miss}	$> 12\,\mathrm{GeV}$	$> 12\,\mathrm{GeV}$
D_{track}	> 0.5 for $\theta_e > 45^\circ$	> 0.5
P_T^l	$> 10\,\mathrm{GeV}$	$> 10\,\mathrm{GeV}$
θ_l	$15^\circ < \theta_e < 120^\circ$	$15^\circ < \theta_\mu < 120^\circ$
δ	$5 < \delta < 50\,\mathrm{GeV}$	$< 70\,\mathrm{GeV}$
ϕ_{acop}	$> 20^\circ$	$> 10^\circ$
ξ_l^2	$> 5000\,\mathrm{GeV}^2$ for $P_T < 25\,\mathrm{GeV}$	—
$\frac{V_{\mathrm{ap}}}{V_p}$	< 0.5 (< 0.15 for $P_T^e < 25\,\mathrm{GeV}$)	< 0.5 (< 0.15 for $P_T^{\mathrm{CAL}} < 25\,\mathrm{GeV}$)
D_{jet}	implicit	> 1.0
# isolated μ	0	1
P_T^X	—	$> 12\,\mathrm{GeV}$

Table 2: *Selection criteria for the isolated electron and muon searches.*

Isolated e Candidates	$P_T^X < 12$ GeV	$12 < P_T^X < 25$ GeV	$P_T^X > 25$ GeV
e^-p 208 pb^{-1}	$9/11.3 \pm 1.5$ (54%)	$5/3.4 \pm 0.5$ (62%)	$3/3.2 \pm 0.5$ (69%)
e^+p 296 pb^{-1}	$7/12.6 \pm 1.7$ (68%)	$5/3.9 \pm 0.6$ (72%)	$3/4.0 \pm 0.6$ (77%)
$e^\pm p$ 504 pb^{-1}	$16/23.9 \pm 3.1$ (61%)	$10/7.4 \pm 1.0$ (67%)	$6/7.3 \pm 1.0$ (73%)

Table 3: *Results of the search for events with isolated electrons and missing transverse momentum. The number of observed events is compared to the SM prediction (observed/expected). The fraction of the SM expectation arising from W production is given as a percentage in parentheses. The quoted errors contain statistical and systematic uncertainties added in quadrature.*

Isolated μ Candidates	$12 < P_T^X < 25$ GeV	$P_T^X > 25$ GeV
e^-p 208 pb^{-1}	$1/1.6 \pm 0.3$ (77%)	$2/2.3 \pm 0.4$ (85%)
e^+p 296 pb^{-1}	$2/2.2 \pm 0.3$ (82%)	$3/3.4 \pm 0.5$ (81%)
$e^\pm p$ 504 pb^{-1}	$3/3.8 \pm 0.6$ (80%)	$5/5.7 \pm 0.8$ (83%)

Table 4: *Results of the search for events with isolated muons and missing transverse momentum. Other details as in the caption to Table 3.*

Isolated Lepton Candidates	$P_T^X < 12$ GeV	$12 < P_T^X < 25$ GeV	$P_T^X > 25$ GeV
e^-p 208 pb^{-1}	$9/11.3 \pm 1.5$ (54%)	$6/5.1 \pm 0.7$ (67%)	$5/5.5 \pm 0.8$ (75%)
e^+p 296 pb^{-1}	$7/12.6 \pm 1.7$ (68%)	$7/6.2 \pm 0.9$ (75%)	$6/7.4 \pm 1.0$ (79%)
$e^\pm p$ 504 pb^{-1}	$16/23.9 \pm 3.1$ (61%)	$13/11.2 \pm 1.5$ (71%)	$11/12.9 \pm 1.7$ (77%)

Table 5: *Results of the search for events with isolated electrons or muons and missing transverse momentum. Other details as in the caption to Table 3.*

Process	$P_T^X >$ (GeV)	$\langle\sqrt{s}\rangle$ (GeV)	σ (pb)	$\sigma_{\rm SM}$ (pb)
$ep \to lWX$ $W \to e\nu_e$	0	316	$0.090^{+0.032}_{-0.028}$ (stat.) $^{+0.013}_{-0.013}$ (syst.)	0.13
$ep \to lWX$ $W \to \mu\nu_\mu$	12	316	$0.044^{+0.022}_{-0.018}$ (stat.) $^{+0.006}_{-0.006}$ (syst.)	0.05
$e^+p \to lWX$	0	315	$0.82^{+0.31}_{-0.26}$ (stat.) $^{+0.08}_{-0.08}$ (syst.)	1.2
$e^-p \to lWX$	0	318	$1.03^{+0.45}_{-0.38}$ (stat.) $^{+0.16}_{-0.16}$ (syst.)	1.3
$ep \to lWX$	0	316	$0.89^{+0.25}_{-0.22}$ (stat.) $^{+0.10}_{-0.10}$ (syst.)	1.2

Table 6: *Extracted W production cross sections. The predicted SM cross section, $\sigma_{\rm SM}$, is given in the last column and has an estimated uncertainty of $\pm 15\%$.*

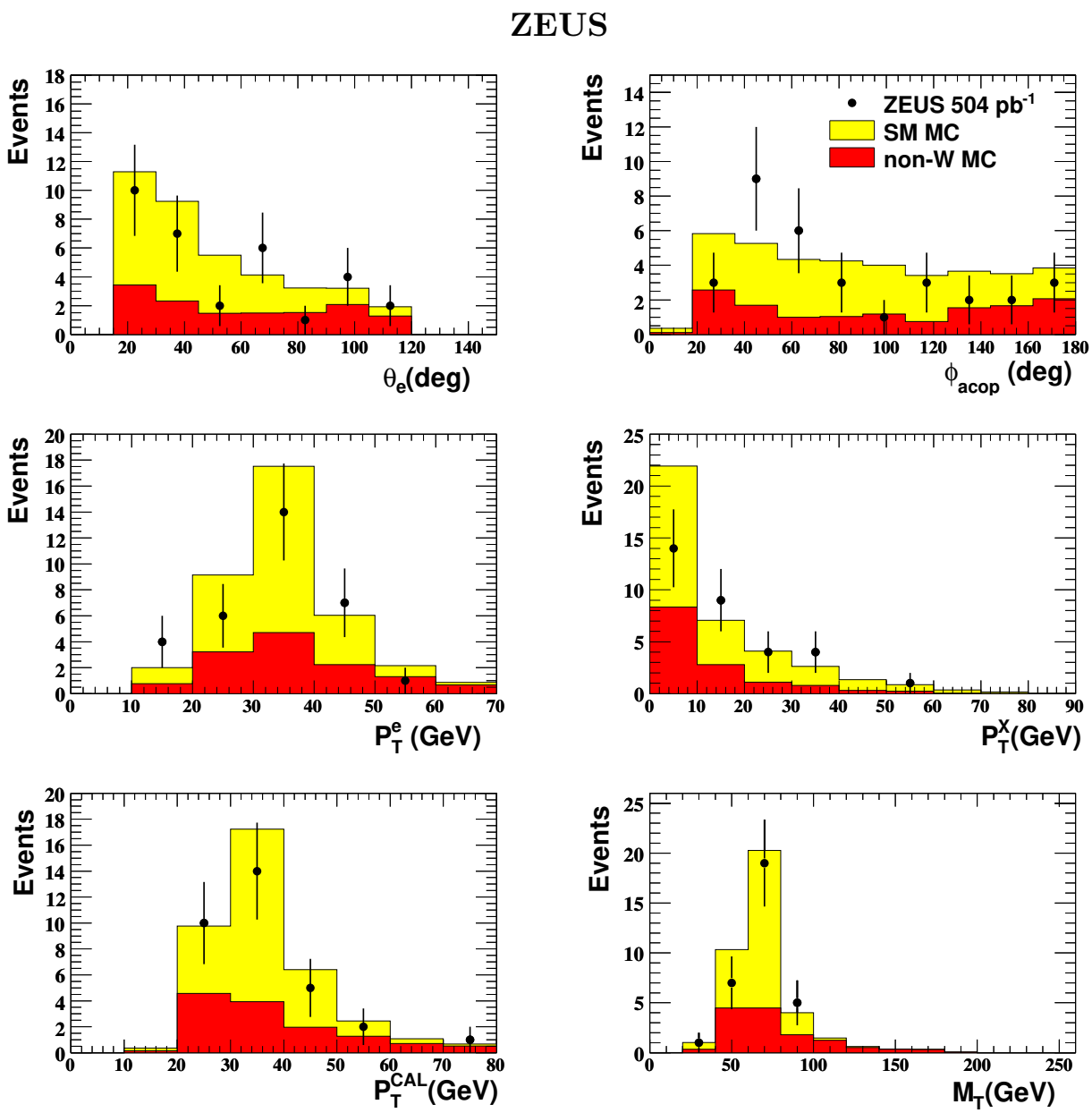

Figure 1: *Distributions of the isolated electron events (points) compared to the SM expectation for the $e^{\pm}p$ collision data. The light-shaded histogram represents the Standard Model MC prediction, the dark shaded area being the prediction for events not arising from $ep \to lWX$. The error bars on the data points correspond to $\sqrt{N}$ where N is the number of events. The variables shown are described in detail in the text.*

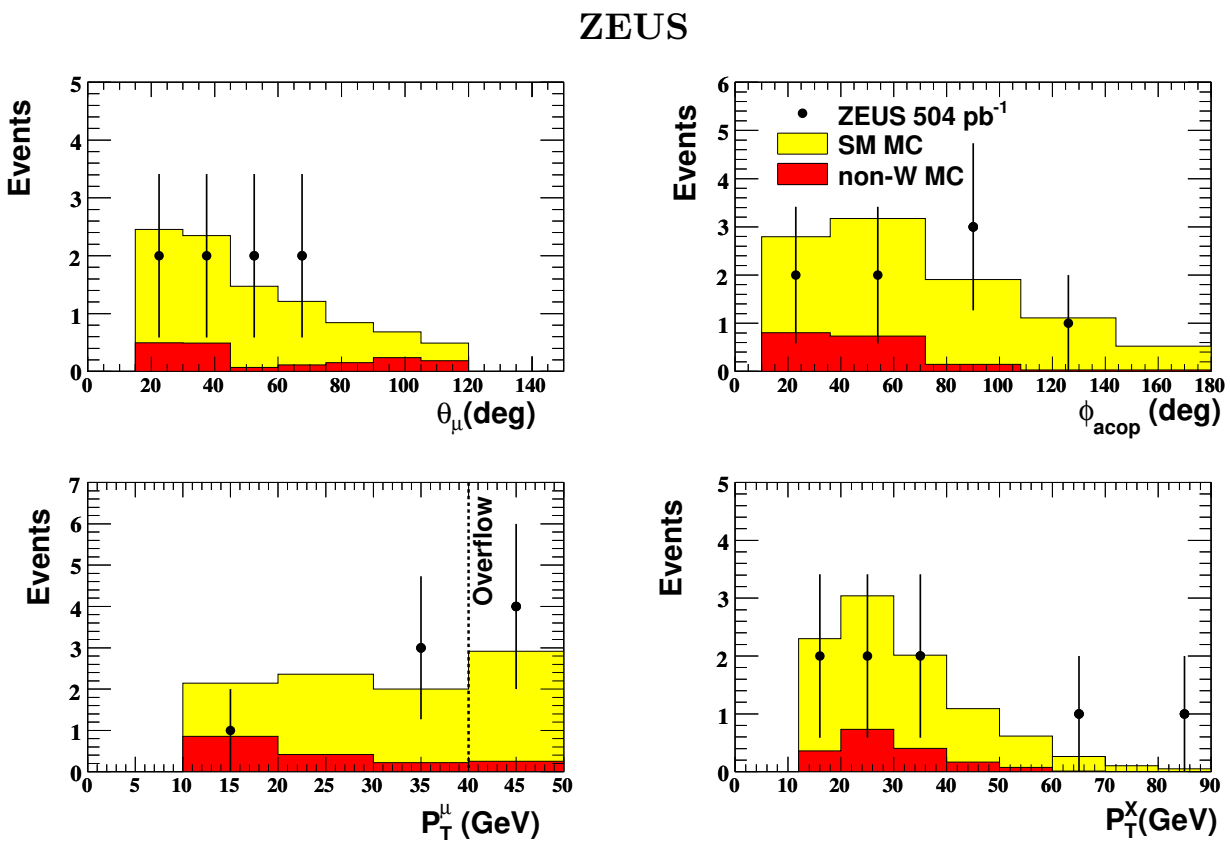

Figure 2: *Isolated muon data (points) compared to the SM expectation for the $e^{\pm}p$ collision data. For $P_T^\mu > 50\,\mathrm{GeV}$ the resolution of tracking used becomes significant compared to the bin width, such events have been grouped together in the overflow bin in this figure. Other details as in the caption to Fig. 1.*

A Full likelihood distribution

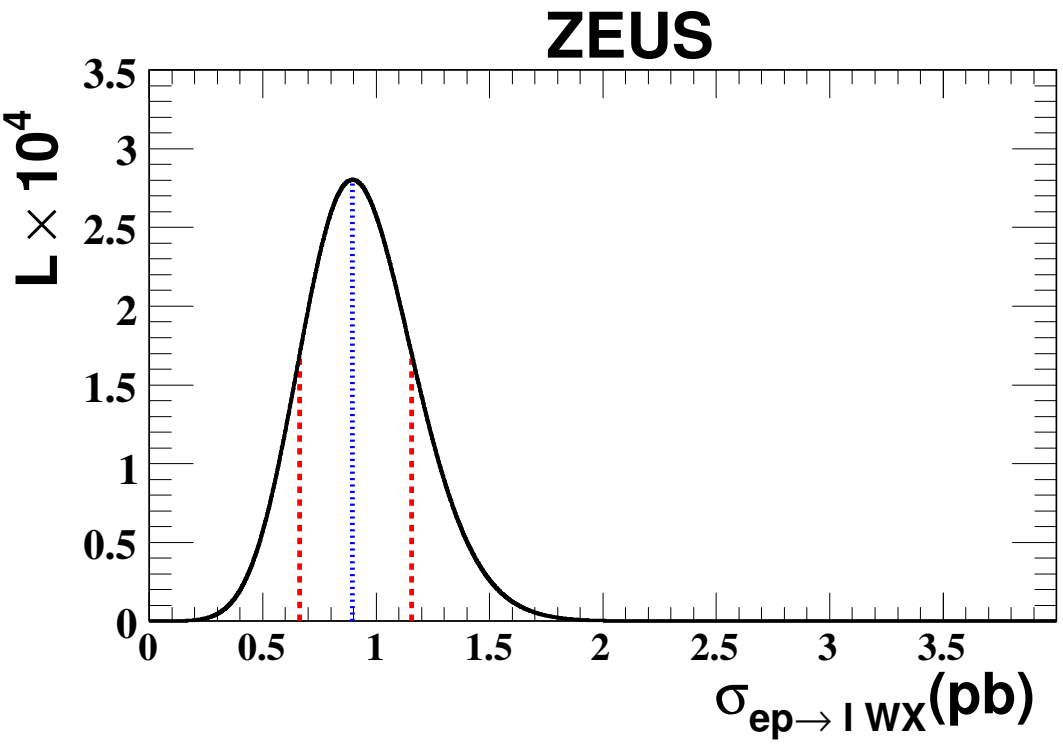

Figure 3: *Full likelihood distribution, including systematic uncertainties, for $\sigma_{ep\to lWX}$. The dotted line indicates the central value of the cross section, the dashed lines indicate the upper and lower bounds on the cross section.*